Adsorption at the Interface between Water and Self-Assembled Monolayers: Structure and Electronic Spectra

John Vieceli and Ilan Benjamin*

Department of Chemistry and Biochemistry, University of California, Santa Cruz, California 95064

Received: January 11, 2002; In Final Form: April 22, 2002

The structure of the interface between water and self-assembled organic monolayers having different roughness and polarity is investigated by molecular dynamics computer simulations. The electronic absorption spectrum of an adsorbed chromophore at these different interfaces is computed and correlated with the structure of the interface. Several different electronic transitions characterized by different changes in the electric dipole moment are considered. We find that the effective polarity of the interface is greater than that of bulk water in contrast to the situation at several liquid/liquid interfaces, but in agreement with recent experiments at the liquid/solid interface. We show that this higher effective polarity is due to a contribution from the polar groups at the surface that is larger than the loss due to the decreased interaction with water.

I. Introduction

Solvent polarity, structure, and dynamics at the liquid/liquid[1] and liquid/solid[2] interfaces may be different from the properties of the bulk solvent and this in turn may have a marked effect on solute behavior and chemical reactivity. Unfortunately, experimental studies of solvation and reactions at liquid/liquid and liquid/solid interfaces are difficult because of the buried nature of the interface. This results in two major problems: lack of basic knowledge about the structure of the interface and complications due to the effect of the two adjoining bulk phases. Both problems make the interpretation of experimental measurements difficult. While in recent years advances in nonlinear optical spectroscopies and other surface sensitive techniques have enabled us to make great progress,[3,4] there are still many open issues that are almost all related to the correct microscopic description of the interface. For example, the shift in the electronic spectrum of a chromophore adsorbed at the liquid/liquid[5] and liquid/solid[6] interfaces can be used to obtain valuable information about the degree of intermolecular interaction at the interface relative to the bulk, but correlating this information to specific structural motifs is still an open problem.

One important difference between the liquid/liquid and liquid/solid interfaces is the existence of thermally excited capillary fluctuations and partial mixing of the two liquids in the former. A solute adsorbed at the liquid/liquid interface may have a mixed solvation shell structure whose composition may sensitively depend on the location of the solute. While this feature is an integral part of this environment and has been studied by molecular dynamics simulations,[1] it would be useful to understand the contribution of the intrinsic interface to solvation, spectroscopy, and chemical reactivity in a way that is better controlled experimentally. Studies at the liquid/nonmetallic solid interface are one way in which this can be done.

Another approach which we have recently been exploring is to study the contribution of the intrinsic structure of the interface between a liquid and another phase by examining the interface between water and self-assembled organic monolayers. Besides the independent importance of this molecular system for applied science and technology, it enables us to study spectroscopy, solvation, and reactions at an interface whose microscopic structure is well characterized (like a solid−surface), yet still exhibits many of the unique features of a liquid/liquid interface.

In previous publications,[7,8] we have examined the interface between water and self-assembled hydrocarbon chains attached to a silica surface in order to understand the effect of surface roughness on the structure of water and the spectroscopy of adsorbed chromophores. In the present paper we begin a program to systematically modify the chemical nature of this interface, to produce surfaces with different polarities. This will allow for a better understanding of the nature of the interactions at the liquid/liquid as well as the liquid/solid interfaces in a system that can be more easily studied experimentally.

The design and preparation of self-assembled monolayers with well characterized molecular structure[9,10] and, in particular, those made of long-chain hydrocarbons that are either physisorbed on a solid surface like graphite[10] or chemically attached to a metal or silica surface[11] is well-known. The ability to design the chains with a particular terminal chemical group such as OH, SH, S, Cl, COOH, or NH_2 is important for the objective of our studies because one obtains surfaces with rich structures and varied physiochemical properties. The interface between these systems and water can be investigated by a STM[10] (scanning tunneling microscope), an AFM[10] (atomic force microscope), neutron reflection,[12] electrochemical techniques, and other thermodynamic and surface characterization methods, such as wetting experiments[13] and nonlinear spectroscopic techniques.[14] Self-assembled monolayers with different electronic and molecular structures have been used in recent years to study a number of different molecular processes, such as electron transmission,[15] energy transfer, and spectroscopy.[16]

In this paper, we consider the interface between water and five different self-assembled hydrocarbon monolayers. Some or all of the top methyl groups of each monolayer have been substituted by a chlorine atom, which is partially negatively charged. The five different systems are also designed to have different degrees of roughness by using different length hydrocarbon chains and changing the ratio of the short to long chains. Thus we obtain surfaces with different polarity and

* Corresponding author.

10.1021/jp020068w CCC: $22.00
Published on Web 07/24/2002

roughness that provide a mimic to the water/1,2-dichloroethane and water/carbon tetrachloride interfaces. A chromophore adsorbed at these interfaces will be partially solvated by water to a degree that will depend on the roughness of the surface and its polarity and will also interact with the organic phase. We compute the electronic absorption spectrum of this chromophore for a number of electronic transitions distinguished by different changes in the dipole moment and try to find a direct correlation between the spectral shift and the structure of the interface. Although several molecular dynamics studies of water/membrane interfaces and of self-assembled monolayers have been reported,[17−24] none (other than the previous work from our group[8]) has been reported for the spectroscopy and reactivity of adsorbed and covalently attached chromophores at the interface between water and self-assembled monolayers.

We find that the polarity of the interface, as characterized by the shift in the electronic absorption spectrum of the chromophore, is greater than that of bulk water. This is in contrast with the situation found in experiments and simulations of solvatochromism at several liquid/liquid interfaces. However, this finding is in agreement with recent experiments at the liquid/solid interface.[6] We show that this higher effective polarity is due to a contribution from the polar groups at the surface that more than compensate for the loss due to decreased interaction with water. Direct correlation is found between the effective polarity and the roughness of the interface.

The rest of the paper is organized as follows. In Section II we discuss the five different interfaces studied including the choice of the potential energy functions. In Section III we discuss the methods used to characterize the structure and compute the electronic spectra. In Section IV we discuss the results of the structure determination and the electronic spectral shift. Conclusions are presented in Section V.

II. System and Potential Energy Functions

A. Potential Energy Functions. In general, we use pairwise additive intermolecular potentials which are summed over all pairs of sites

$$U(\mathbf{r}) = \sum_{i<j} 4\epsilon_{ij}\left[\left(\frac{\sigma_{ij}}{r_{ij}}\right)^{12} - \left(\frac{\sigma_{ij}}{r_{ij}}\right)^{6}\right] + \frac{q_i q_j}{r_{ij}} \qquad (1)$$

where r_{ij} is the distance between sites i and j, which are in two different molecules, q_i and q_j are the fixed charges on sites i and j, and the Lennard-Jones parameters σ_{ij} and ϵ_{ij} are determined from the parameters of the individual sites according to the usual combination rules for mixtures[25]

$$\sigma_{ij} = \frac{1}{2}(\sigma_i + \sigma_j), \quad \epsilon_{ij} = \sqrt{\epsilon_i \epsilon_j} \qquad (2)$$

In recent years, there have been a number of papers demonstrating the importance of including many-body polarizable potentials for accurate calculation of the adsorption free energies and hydration structure.[26−29] We have also recently demonstrated that polarizable potentials could make important contributions to electronic spectral shifts involving large changes in the dipole moment.[30] Nevertheless, we chose to use nonpolarizable potentials in this work for two reasons: (1) to compare the results with published liquid/liquid interface work which also uses nonpolarizable potentials; (2) to have a consistent model for examining both structure and spectra (in the present paper), and dynamic solvent effect as well as electron transfer (in a subsequent paper). We plan on examining the importance of polarizable potentials in these systems soon.

TABLE 1: The Number of Each Hydrocarbon Molecule Used To Construct the Five Monolayers

monolayer	$C_{18}H_{37}$	$C_{17}H_{34}Cl$	$C_{22}H_{45}$	$C_{21}H_{42}Cl$
smooth-all-Cl		100		
smooth-mix-Cl	50	50		
rough-all-Cl		50		50
rough-out-Cl	50			50
rough-in-Cl		50	50	

TABLE 2: The Lennard-Jones and Coulombic Potential Energy Parameters for Intramolecular and Intermolecular Interactions

atom or group	σ (Å)	ϵ (kcal/mol)	Q (e)
intramolecular, nonbonded	4.0	0.100	
CH_2	3.905	0.118	0.0
CH_3	3.905	0.175	0.0
CH_2 (bonded to Cl)	3.980	0.114	+0.227
Cl	3.160	0.500	−0.227
O	3.166	0.155	−0.82
H	0.0	0.0	+0.41
solute	5.154	0.1104	$\pm Q_n$

A.1. Organic Monolayers. We study five different self-assembled monolayers characterized by different structure and polarity. Each system includes 100 hydrocarbon molecules covalently attached at one end to a Si−O bond of a silica surface. The Si atoms are arranged on a two-dimensional square lattice with a distance of 4.3 Å between neighboring atoms, generating a 43 Å × 43 Å surface. Four different hydrocarbon molecules are used, which include two methyl-terminated hydrocarbons, $C_{18}H_{37}$ and $C_{22}H_{45}$, and two chlorine-terminated hydrocarbons, $C_{17}H_{34}Cl$ and $C_{21}H_{42}Cl$, to construct the five different monolayer surfaces. Different surface structure and polarity is generated by varying the ratio of short to long hydrocarbons and the number of chlorine-terminated hydrocarbons present on a surface. Recognizing that a large number of surfaces can be designed, the focus of this study is on the five monolayers described in Table 1. Since self-aggregation of hydrocarbon molecules is not observed experimentally,[7] different hydrocarbon types are randomly attached to the silica surface. (Conditions where self-aggregation occurs are possible but these can be controlled.[31])

Each hydrocarbon molecule consists of a chain of CH_2 groups, modeled as a united atom of mass 14, terminated by either a CH_3 group, modeled as a united atom of mass 15, or a chlorine atom. The intramolecular potential is fully flexible and includes harmonic bending and stretching terms and a 3-term Fourier series for the torsional energy. The harmonic force constants, equilibrium bond lengths and angles and torsional parameters are taken from the Amber force field[32] and Jorgensen's TIPS parameters.[33] The intramolecular nonbonded interactions for two atomic centers separated by three or more bonds are modeled using a Lennard-Jones potential. The parameters are the same as those used in the previous work on hydrocarbon chains,[8] and are given in Table 2. The interaction energy is scaled down by a factor of 2 for the 1,4 atoms in each chain.[34] The intermolecular potential between the hydrocarbon molecules is also described using the Lennard-Jones function, but in addition there is a Coulombic term between every pair of charged atoms in the system. The charges and the Lennard-Jones parameters of the chlorine atoms, shown in Table 2, are selected to be the same as those used in our study of the water/1,2-dichloroethane interface[35] for the reasons discussed in the Introduction.

A.2. Water and Water−Organic Monolayer Interactions. The system includes 1000 water molecules on one side of the self-assembled monolayer. The potential energy function for the water is based on the SPC model[36] with the spectroscopic intramolecular potential energy function of Kuchitsu and Morino.[37] The explicit form of the potential used is given by

$$U_{H_2O} = \frac{1}{2}[2211(x^4 + y^4) + 114.8(x^3y + xy^3) + 186.6x^2y^2 - 244.04(x^2z^2 + y^2z^2) - 71.78xyz^2 - 1371(x^3 + y^3) - 20.10z^3 - 45.94(x^2y + xy^2) + 22.97(x^2z + y^2z) + 21.53(xz^2 + yz^2) - 94.75xyz + 1214(x^2 + y^2) + 109.2z^2 - 29.00xy + 65.46(xz + yz)] \quad (3)$$

where x and y represent the deviation in the two OH bond lengths from equilibrium, z represents the deviation from the equilibrium bond angle (in radians), and the coefficients are given in units of kcal/mol and Å. The potential energy between the water and the hydrocarbon molecules is modeled using Lennard-Jones and Coulombic potentials for each pair of atoms. The parameters used to describe these interactions for the water atoms are given in Table 2.

A.3. Chromophore. The chromophore is modeled as two atoms held at a fixed distance (using A SHAKE type constraint[38]) of either 6 or 8 Å, which is a typical charge separation in large dye molecules.[39] The charges on the solute atoms, $\pm Q_n$, depend on the electronic state n of the chromophore. In the previous study of methyl-terminated monolayers,[8] the chromophore was covalently attached to a terminal hydrocarbon atom, which established the effect of surface roughness and exposure to water on the electronic spectra and solvent dynamics. However, the focus of this study is to design different surfaces and determine their effect on the interface structure and electronic spectra while the chromophore freely translates and rotates in the interface region. Because of this, during the simulation, the chromophore may desorb from the surface and diffuse to the bulk water. To increase the sampling of surface configurations we have added an external window potential which acts on the chromophore center of mass and is given by

$$U_{win}(z_I) = kH(\zeta)\zeta^3$$

$$\zeta = |z_I - c - Z_{c.m.}| - \frac{1}{2}w \quad (4)$$

where H is the unit step function [$H(\zeta) = 0$ for $\zeta \le 0$ and $H(\zeta) = 1$ for $\zeta > 0$], z_I is the coordinate of the chromophore center of mass along the axis normal to the interface plane, $Z_{c.m.}$ is the coordinate of the system center of mass along the axis normal to the interface plane, c is the center of the window relative to $Z_{c.m.}$, w is the width of the window (12 Å), and k is chosen to be 2390 (kcal/mol) Å^{-3}. This potential does not interact with the chromophore while it is adsorbed to the monolayer and thus does not affect any of the results of interest. In fact, the window potential was present during the simulations but it rarely turned on due to the stability of the chromophore in the interface region. The interaction of the chromophore with the water and hydrocarbon atoms is modeled using a sum of Lennard-Jones and Coulombic potentials. The chromophore parameters for the Lennard-Jones potential are taken from the previous publication on methyl-terminated self-assembled monolayers[8] and are given in Table 2.

B. Boundary Conditions. Because of the geometry of our system, periodic boundary conditions are used in the plane parallel to the surface but not in the direction normal to the interface. This creates a water liquid/vapor interface on one end. A reflecting wall is placed in the vapor phase at a distance of approximately 30 Å from the water liquid/vapor interface to prevent the escape of gas-phase water molecules and maintain a fixed vapor pressure.

All of the intermolecular interactions calculated are smoothly switched to zero using a switching function when the distance between two atoms is between 19.5 and 21.5 Å.[40] The use of a continuous switching function at the largest possible cutoff distance (consistent with the periodic boundary conditions) should minimize errors due to the neglect of long-range forces. An estimate of these forces using a uniform reaction field method (by surrounding the water lamella with an infinite medium of dielectric constant equal to 78) shows only a small contribution (less than 1%) to the chromophore−water interaction energy (most of it comes from first shell water molecules). Although a more sophisticated, two-dimensional Ewald sum[41] method can be applied to the geometry of our system, it is not clear what the implications are when the inhomogeneous charge distribution at the interface is extended infinitely, thus magnifying surface fluctuations. However, an application of the three-dimensional Ewald method to the water/1,2-dichloroethane interface of approximately the same size shows only minor effects on the structure of interfacial water molecules (unpublished results). Thus, it would be useful in the future to examine this issue in greater detail.

III. Methods

A. Electronic Spectra. The molecular dynamics methodology of spectral shift calculations has been previously discussed and is only briefly outlined below.[42,8] The total Hamiltonian for the system in the nth electronic state is written as

$$H_n = H_0 + \Delta E_n + Q_n\Gamma(\mathbf{r}) \quad (5)$$

In eq 5, H_0 is the Hamiltonian for the hydrocarbon chains, water, hydrocarbon−water interactions, and nonelectrostatic interactions between the chromophore and all other atoms in the system, ΔE_n is the fixed gas-phase zero point energy of the nth electronic state, Q_n is the atomic charge of the solute atoms and

$$\Gamma(\mathbf{r}) = \sum_i q_i[(|\mathbf{r}_i - \mathbf{r}_A|)^{-1} - (|\mathbf{r}_i - \mathbf{r}_B|)^{-1}] \quad (6)$$

In eq 6, q_i and $\mathbf{r}_i$ are the charge and position of the ith liquid atom, respectively, and $\mathbf{r}_A$ and $\mathbf{r}_B$ are the positions of the positively and negatively charged solute atoms, respectively. To calculate the absorption spectrum, the classical Franck−Condon approximation is used assuming the transition dipole moment is independent of solute and solvent positions. The energy difference between the chromophore in ground state α and excited state β at a given atomic configuration $\mathbf{r}$ is written as

$$\hbar\Omega(\mathbf{r}) = H_\beta - H_\alpha = \Delta E_\beta - \Delta E_\alpha + (Q_\beta - Q_\alpha)\Gamma(\mathbf{r}) \quad (7)$$

The absorption spectrum $I_{\alpha\beta}$ for the transition $\alpha \rightarrow \beta$ corresponds to the equilibrium probability distribution of the transition frequencies and is given by

$$I_{\alpha\beta}(\omega) = \langle\delta[\omega - \Omega(\mathbf{r})]\rangle_\alpha = \frac{\int\delta[\omega - \Omega(\mathbf{r})]e^{-H_\alpha/kT}\,d\mathbf{r}}{\int e^{-H_\alpha/kT}\,d\mathbf{r}} \quad (8)$$

TABLE 3: The Different Electronic Transitions Determined Given the Initial Dipole and the Overall Change in Dipole

transition number	R (Å)	$\pm Q$ (e)	μ_{initial} (D)	$\Delta\mu$ (D)
0	6.0	0.0	0.0	+14.4
1	6.0	0.5	14.4	−14.4
2	6.0	0.667	19.2	−19.2
3	8.0	0.5	19.2	−19.2
4	6.0	1.0	28.8	−28.8

where δ is the Dirac delta function, k is Boltzmann's constant, and T is the temperature. Since the solvent degrees of freedom are at equilibrium with the solute in state α and our potentials are nonpolarizable, an equilibrium simulation in this state enables us to calculate the spectrum for a transition from the state α to any other electronic state β by simply binning $Q_\alpha\Gamma(\mathbf{r})$ and using the relation: $\hbar\Omega(\mathbf{r}) = \Delta E_\beta - \Delta E_\alpha + (Q_\beta/Q_\alpha - 1)Q_\alpha\Gamma(\mathbf{r})$. The absorption line shape is fit to a Gaussian function, which yields the peak position, $\Delta\omega$, for $I_{\alpha\beta}$. Due to the pairwise additive nature of the system model, $\Delta\omega$ can be written as a sum of contributions from the monolayer, $\Delta\omega^{\text{int er}}_{\text{monolayer}}$, and the water, $\Delta\omega^{\text{int er}}_{\text{aq}}$,

$$\Delta\omega = \Delta\omega^{\text{int er}}_{\text{monolayer}} + \Delta\omega^{\text{int er}}_{\text{aq}} \tag{9}$$

Another property of interest in these systems is the contribution from water to the spectral shift peak position relative to the same transition in bulk water

$$s_{\text{aq}} = \Delta\omega^{\text{int er}}_{\text{aq}}/\Delta\omega^{\text{bulk}}_{\text{aq}} \tag{10}$$

B. Interface Structure. Since the system essentially consists of water next to a surface with varying polarity and roughness, it is of interest to determine the effect of the different monolayers on the structure of water. This information will be used later to understand the variations in the electronic spectra of the adsorbed chromophore. The characterization of the interface structure follows the method used elsewhere[35] (for the water/1,2-dichloroethane interface and is based on the procedure of Linse[43] and Meyer et al.[44]). Since the hydrocarbon molecules lack significant lateral and transverse mobility, the interface structure is determined by the equilibrium fluctuations in the water around the monolayer surface. During the molecular dynamics simulation, the XY plane, with cross section S (43 Å × 43 Å), is divided into $N \times N$ squares generating an array of N^2 columns each with cross section S/N^2. N is a variable selected to be 1, 2, 4, and 6, such that $\sqrt{S}/N > \xi_b$, where ξ_b is the water bulk correlation length[25] (about 5 Å). At each time step, the Z_{ij} position of oxygen from water with the minimum value in the ijth column is binned to generate a probability distribution for observing a particular minimum Z value, $P_N(Z)$. The average minimum Z value for the oxygen of water over the trajectory of length T is

$$\langle Z_N\rangle = \frac{1}{N^2}\sum_{i,j}\frac{1}{T}\int_0^T Z_{ij}(t)\,\mathrm{d}t \tag{11}$$

This procedure and the limit on the value of N averages out fluctuations smaller than ξ_b. Additionally, the time scale over which the fluctuations in $\langle Z_N\rangle$ decay to the average value can be determined using an equilibrium time correlation function; however, these results are applicable to solvent dynamics to be discussed in a future publication.

C. Simulation Details. Electronic spectra are determined for the transitions shown in Table 3 at each of the five surfaces (Table 1). Specifically, the two cases with an overall change in dipole of −19.2 D are used to test the effect of a 33% increase in the overall change in dipole from −14.4 D (Transition 1) on the spectral shift, with one increase due to ground state charge magnitude (Transition 2) and the other due to ground state charge separation (Transition 3). Each chromophore electronic state is equilibrated at each of the five surfaces until the solute electrostatic interaction energy with the water and the monolayer is stable, which requires 10 ps. Following the equilibration, a 100 ps equilibrium simulation is run to calculate the structural properties of the interface and electronic spectrum. This time was found to be sufficient for obtaining convergent absorption spectrum. The calculations are performed using the velocity version[40] of the Verlet algorithm and an integration time step of 0.5 fs at 300 K. The total simulation time of 2.5 ns (100 ps for each of 25 different systems) takes 104 days on two dual processor Pentium III 800 MHz computers.

IV. Results and Discussion

In the first section (Section IV.A) a structural analysis of the systems is discussed to understand the differences between the surfaces and how these differences affect the water and chromophore. In Section IV.B, this structural analysis is related to the spectra of the chromophore for different electronic transitions at each of the five surfaces. In Section IV.C, the applicability of continuum electrostatic models to these systems is discussed.

A. Interface Structure. *1. Organic Monolayer Structure.* The most obvious difference between the surfaces is their roughness. In the case of the two smooth surfaces, the average Z position of the terminal hydrocarbon atom is 20.4 Å, where $Z = 0$ Å is the position of the carbon atom attached to the silica surface. The three rough surfaces also have short chains, with an average terminal hydrocarbon atom Z position of 20.5 Å, and long chains with an average of 24.9 Å, which creates 4.5 Å pockets on the monolayer surface that may be occupied by water molecules.

An important property that characterizes the monolayer structure is the tilt angle, θ, between the hydrocarbon end-to-end vector and the interface normal. The top two panels of Figure 1 show the probability densities of θ for the two smooth surfaces (A) and the three rough surfaces (B). The tilt angle probability density for the 100% chlorinated smooth surface (which will be referred to as smooth-all-Cl) is the most strongly peaked at 19° (thick solid line in panel A). The increased width observed when only 50% of the smooth surface is chlorinated (smooth-mix-Cl, thin line in panel A) is due to the introduction of methyl-terminated hydrocarbons with a smaller θ value on average. This is consistent with the results from previous simulations[7] with smooth methyl-terminated monolayers where the θ distribution ranges from 0° to 10°. The chlorine-terminated hydrocarbons have a slightly larger value of θ. This results in an increased exposure of the chlorine atoms to adjacent water molecules and thus a more favorable electrostatic interaction. In general, the rough surfaces (panel B) exhibit broader probability densities relative to the smooth surfaces, with the broadest being the 100% chlorinated surface (rough-all-Cl, thick line in panel B). The two rough surfaces which are 50% chlorinated (with the chlorine attached to the short hydrocarbon chain, rough-in-Cl or to the long hydrocarbon chain, rough-out-Cl) are similar to the smooth-all-Cl surface with a slight shoulder toward lower θ values.

The torsional angle, ϕ, probability distribution is another important structural feature that is influencing the tilt angle and thus can provide additional insight into the observed broader

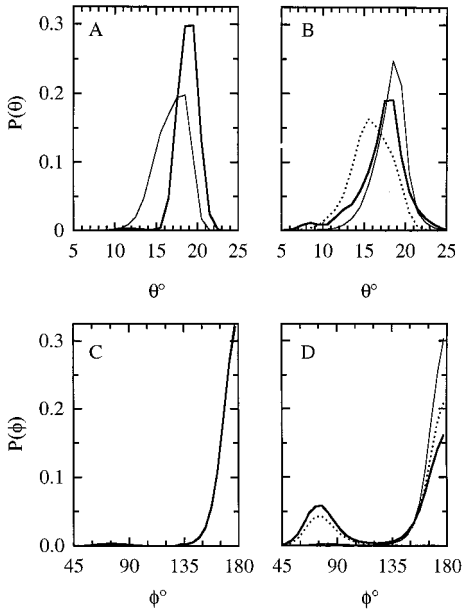

Figure 1. The equilibrium structure of the five self-assembled monolayers. (A) The probability densities for the angle between the hydrocarbon end-to-end vector and the interface normal for the smooth-all-Cl (thick line) and smooth-mix-Cl (thin line) surfaces. (B) Same as A for the rough-all-Cl (thick line), rough-out-Cl (dotted line), and rough-in-Cl (thin line) surfaces. (C) The probability distributions of the torsional angle defined by the top four atoms of each chain for the two smooth surfaces with the lines the same as A. (D) Same as C for the long hydrocarbon molecule on the rough surfaces with the lines the same as B.

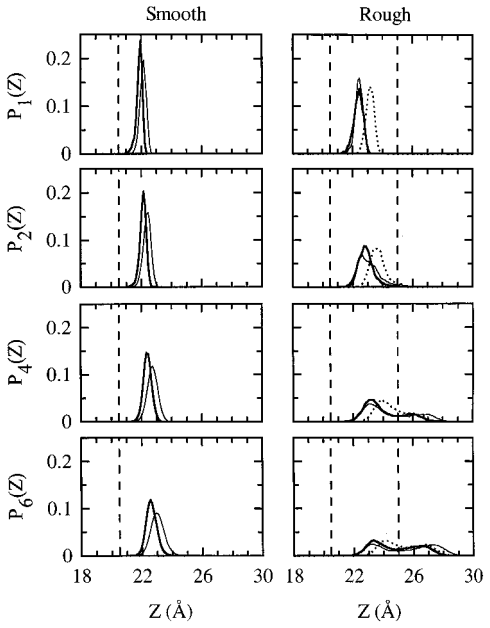

Figure 2. The equilibrium structure of water described by P_N *(Z)* for N values of 1, 2, 4, and 6 separated by smooth (left panels) and rough (right panels) surfaces. Smooth surfaces: smooth-all-Cl (thick line), smooth-mix-Cl (thin line). Rough surfaces: rough-all-Cl (thick line), rough-out-Cl (dotted line), rough-in-Cl (thin line). The dashed vertical lines at 20.5 and 25.0 Å correspond to the average values of the short and long hydrocarbon molecules, respectively.

tilt angle distributions for the rough surfaces. This torsional angle is defined by the top four atoms of each chain. The bottom two panels of Figure 1 show the ϕ distributions for the two smooth surfaces (C) and the long hydrocarbon molecules of the three rough surfaces (D). The ϕ distributions of the short hydrocarbon molecules on the rough surfaces are not shown since the data is similar to the smooth surfaces. While the terminal torsional angle is primarily in an anti conformation in these systems, the presence of $C_{21}H_{42}Cl$ hydrocarbon molecules on the rough-all-Cl and the rough-out-Cl surfaces gives rise to a population of gauche defects not observed with the rough-in-Cl surface or the two smooth surfaces. The unique behavior of $C_{21}H_{42}Cl$ on these two surfaces is attributed to neighboring short chain hydrocarbons allowing for more freedom in the torsional angle so that the electrostatic interaction energy with water is more favorable.

In conclusion, Figure 1 shows that the smooth surfaces are flat and ordered while the rough surfaces are disordered to a degree that depends on the level of exposure of the polar atoms to water. Thus, both the tilt angle distribution and the percent of gauche defects are affected by the roughness and the percent of chlorination. We will see below that these differences in the monolayer structures are directly related to the structure and orientation of water at the interface.

A.2. Water Structure. It has been previously shown that water better wets rough hydrocarbon surfaces than smooth surfaces[7] and, specifically, there are regions of varying water concentration on the rough hydrocarbon surfaces. Figure 2 demonstrates that this is also the case here for the chlorinated surfaces. This figure shows the probability distributions of the minimum water Z position, P_N *(Z)*, with $N = 1$, 2, 4, and 6 for the smooth (left panels) and for the rough (right panels) surfaces. The average Z positions of the terminal hydrocarbon atoms for $C_{17}H_{34}Cl/C_{18}H_{37}$ and $C_{21}H_{42}Cl/C_{22}H_{45}$ are indicated as vertical dashed lines at 20.5 and 25.0 Å, respectively. When $N = 1$, a sharp, peaked distribution for all five surfaces is observed with averages in the range of 22−23 Å indicating minor water structural differences exist when the entire cross section of each surface is considered. More pronounced differences in the surfaces are evident as N increases and smaller cross sections are considered. The two smooth surfaces maintain strongly peaked distributions that are slightly broader relative to $N = 1$, indicating these interfaces are molecularly sharp and flat. This is consistent with the equilibrium structure of the smooth monolayers presented in panels A and C of Figure 1. The minor differences between smooth-all-Cl and smooth-mix-Cl for all N values are attributed to increased van der Waals and Coulombic forces in the case of the former. In contrast, as N increases for the three rough surfaces, the strongly peaked distributions broaden until almost equal bimodal distributions are exhibited with $N = 6$. The two populations correspond to regions of the surfaces where the minimum water Z position is adjacent to either a short or long hydrocarbon molecule. As with the smooth surfaces, differences in P_N *(Z)* for the rough surfaces are based on whether the water is adjacent to methyl- or chlorine-terminated hydrocarbons.

While Figure 2 demonstrates that the structure of water at this interface is determined by surface roughness, the orientation of water is determined by both the surface roughness and the polarity of the nearby hydrocarbon molecules. The water orientation is described by the probability distributions of the angle χ between the water dipole vector and the interface normal (0° corresponds to the dipole vector parallel to the interface normal where the oxygen atom is closer to the monolayer than the two hydrogen atoms) and the angle ψ between the water O−H vector and the interface normal (0° corresponds to the O−H vector parallel to the interface normal where the oxygen atom is closer to the monolayer than the hydrogen) as a function of water position along the interface normal. Panels A, B, C, and D of Figure 3 correspond to water molecules in the first

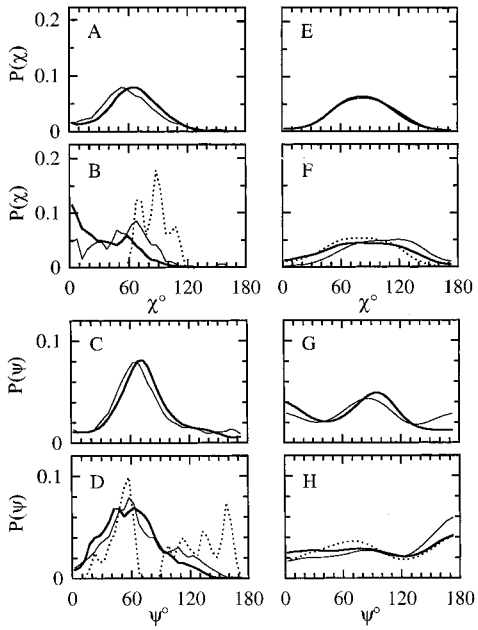

Figure 3. The equilibrium orientation of water. (A) The probability distributions of the angle χ between the water dipole vector and the interface normal corresponding to water in the first layer (20−22 Å) for the smooth-all-Cl (thick line) and smooth-mix-Cl (thin line) surfaces. (B) Same as A for the rough-all-Cl (thick line), rough-out-Cl (dotted line), and rough-in-Cl (thin line) surfaces. (C) The probability distributions of the angle ι between the water O−H vector and the interface normal for water in the first layer at the smooth surfaces. Lines are the same as in A. (D) Same as C for the rough surfaces with the lines the same as in B. (E) Same as A for water in the second layer (22−24 Å). (F) Same as B for water in the second layer. (G) Same as C for water in the second layer. (H) Same as D for water in the second layer.

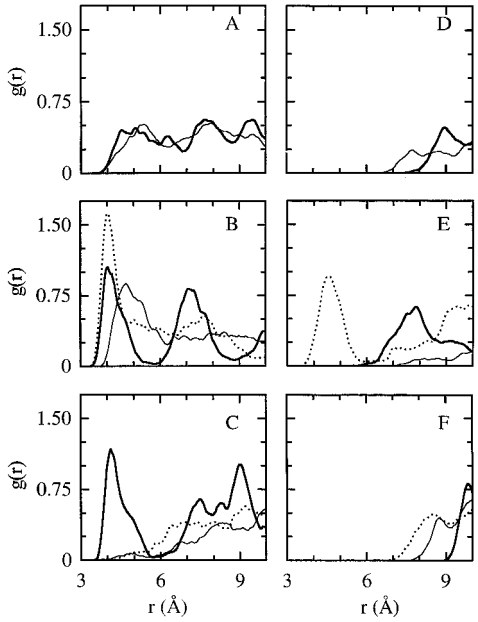

Figure 4. Distribution functions between the solute atoms and the terminal atoms of the hydrocarbon molecules. (A) Positively charged solute atom with terminal atoms at the smooth-all-Cl (thick line) and smooth-mix-Cl (thin line) surfaces. (B) Same as A for the terminal atoms of the long hydrocarbon molecules at the rough-all-Cl (thick line), rough-out-Cl (dotted line), and rough-in-Cl (thin line) surfaces. (C) Same as A for the terminal atoms of the short hydrocarbon molecules at the rough surfaces. Lines are the same as in B. (D) Same as A for the negatively charged solute atom. (E) Same as B for the negatively charged solute atom. (F) Same as C for the negatively charged solute atom.

layer adjacent to the monolayer (20−22 Å) while panels E, F, G, and H correspond to the second layer (22−24 Å). Orientational distributions of water molecules farther into the bulk region are nearly flat, as expected. On the rough surfaces, these two layers of water correspond to molecules located in the surface pockets. Focusing on the first layer, the orientation of water at the smooth surfaces is markedly different from that next to the rough surfaces. On the smooth surfaces, the water dipole (panel A) and the water O−H bond (panel C) distributions, while quite broad, peak on the same plane. This plane forms a 60° angle relative to the surface normal. This is consistent with the tendency of water to maintain its hydrogen bonding network as observed at other water/solid interfaces[45] and it is also indicative of poor surface wetting. In contrast, the rough surfaces show broad distributions of water dipole and water O−H bonds in the 0−100° range with significant populations of O−H bonds pointing toward the surface, indicating surface wetting. Note that water dipoles next to the rough-out-Cl surface peak around 90° which is similar to what is observed at the interface between water and carbon tetrachloride.[46] This demonstrates that the orientation of water at this interface is affected by the polarity of the chlorine atom, so the distribution of water dipoles shifts toward the surface.

For water in the second layer adjacent to the smooth surfaces, panels E and G show the dipole is parallel to the monolayer with one hydrogen atom pointing toward the surface and the other toward the water, which maximizes the possible hydrogen bonding with the surrounding water layers. However, the water in the second layer adjacent to rough surfaces exhibits a more random (bulklike) orientation. While the distribution for the water layer corresponding to the liquid/vapor interface is not shown, the surfaces show results similar to those previously published for the orientation of water at the liquid/vapor interface[47] where the dipole is almost parallel to the interface normal and one hydrogen points toward the liquid while the other hydrogen points toward the vapor.

A.3. Chromophore Adsorption. During the simulations, the chromophore remains adsorbed at the interface, as is reflected by the probability distribution of its center of mass position along the interface normal (data not shown). In general these distributions show translation along the interface normal ranging from 2 to 4 Å over the 100 ps trajectory and translation in the direction perpendicular to the interface normal is of the same magnitude. Since the chromophore is not covalently attached to the surface, it is relatively free to rotate in the interface region. The solute orientation relative to the interface is monitored by probability distributions of the angle between the solute bond vector and the interface normal (0° corresponds to the solute bond vector parallel to the interface normal where the positively charged solute atom is closer to the monolayer than the negatively charged solute atom). These distributions show that angles between 0° and 90° are most probable since the stronger attraction of the positively charged end of the solute to the negatively charged chlorine atoms creates an obvious preferential orientation (see discussion below).

The different interaction of the two solute atoms with the five different surfaces studied here is best described with the aid of the radial distribution functions of the solute atoms with the terminal chain atoms. The left panels of Figure 4 show the distribution functions of the positively charged solute atom with the terminal atoms of the smooth surfaces (panel A), with the terminal atoms of the long hydrocarbon molecules of the rough surfaces (panel B) and with the terminal atoms of the short hydrocarbon molecules of the rough surfaces (panel C). The right panels of Figure 4 (panels D, E, and F) show the same

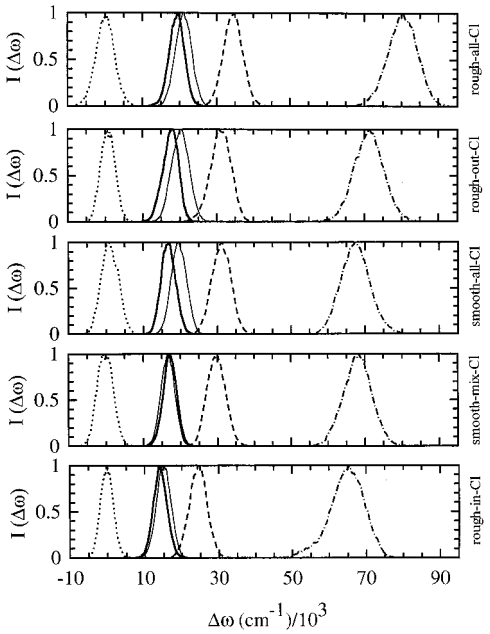

Figure 5. Spectral line shapes for the electronic transitions described in Table 3 relative to the gas phase at each of the five monolayer/water interfaces. The monolayer surface is indicated on the right side of each panel. Dotted lines correspond to Transition 0, thick solid lines to Transition 1, dashed lines to Transition 2, thin solid lines to Transition 3, and dash−dot lines to Transition 4.

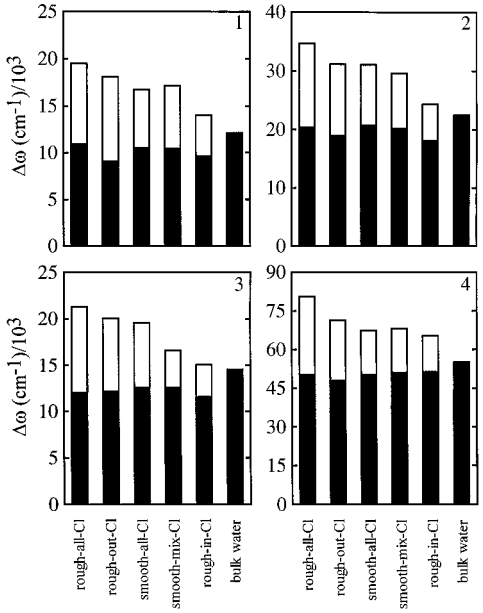

Figure 6. The peak positions from Gaussian fits to the spectral line shapes shown in Figure 5 and the corresponding transitions in bulk water (spectra not shown). The transition number is indicated in the upper right corner of each panel. The contribution to the total spectral shift from the water, $\Delta\omega_{aq}^{int\ er}$, is indicated as the shaded region and the contribution from the monolayer, $\Delta\omega_{monolayer}^{int\ er}$, is indicated as the blank region. Note the different energy axis values in each panel.

data for the negatively charged end of the chromophore. The much smaller and farther away peaks in the right panels compared with the left panels demonstrate that the chromophore is preferentially oriented with the positive end toward the surface.

The more pronounced first peaks in panel B compared with panel A suggest that the chromophore is more strongly interacting with the terminal atoms of the rough surfaces than with the terminal atoms of the smooth surface. This is even the case when one compares the terminal atoms of the short chains in the 100% chlorinated rough surface (thick line in panel C) with the same atoms on the smooth surface (thick line in panel A). This effect is attributed to the different structure of rough and smooth surfaces, where the presence of surface pockets on rough surfaces allows the chromophore atoms to closely approach a larger number of the terminal chains atoms. The interaction of the chromophore with the terminal atoms of the short chains on the two surfaces that are only 50% chlorinated (thin and dotted lines in panel C) is much weaker. We will see that these structural factors play an important role in understanding the electronic spectrum of the chromophore.

In summary, the data in Figures 1−4 show that it is possible to design chlorine-terminated self-assembled monolayers with varying polarity and roughness. The interfaces between these surfaces and water exhibit a range of properties, such as gauche defects, surface wetting, water orientation, and solute adsorption, which can be controlled by varying the composition of the hydrocarbon molecules.

B. Electronic Spectra. We now turn to a detailed discussion of the electronic absorption spectra of the chromophore adsorbed at the different surfaces. In recent years, the shift of the peak position of the electronic spectra relative to that in the bulk phase has been successfully used to assign an effective polarity to the interface region.[5,6,48,49] The hope is that this surface polarity scale is much more useful for understanding surface effects on chemical reactivity and related phenomena than, for example, an interface dielectric constant. The spectral shift is to higher energies ("blue shift") if the excited electronic state involved in the transition is stabilized to a lesser degree than the ground state. Opposite behavior ("red shift") is observed if the excited state is stabilized to a larger degree than the ground state. Since in our case the electronic states are distinguished only by their permanent dipole moment, more polar environments result in larger shifts.

Figure 5 shows the calculated spectral line shapes of the five electronic transitions (listed in Table 3) at the five different monolayer surfaces examined in this work. The energy axis is depicted relative to the gas phase and all the line shapes are normalized to a peak value of 1. The figure demonstrates that each spectrum is well described by a Gaussian function. Figure 6 is a summary of the peak positions of all these transitions showing also the separate contributions from the water (shaded region) and the organic chains (blank region) to the spectral shifts. Several observations can be made from these results:

(1) The peak positions of the spectra for Transition 0 are almost zero (Figure 5) for all of the monolayer surfaces which indicates that immediately following the electronic transition the water molecule dipoles are randomly oriented around the neutral ground-state solute and, in addition, the contribution to the spectral shift from the monolayer is negligible in this case.

(2) For Transitions 1−4, the spectra are blue-shifted relative to the same transitions in the gas phase since the ground-state dipole is greater than the excited state dipole. The peak positions of the spectral shifts at the five chlorine-terminated surfaces and the three methyl-terminated surfaces previously studied[8] yield the following interface polarity order:

$$\text{rough-in-CH}_3 < \text{smooth-CH}_3 < \text{rough-out-CH}_3 < \text{rough-in-Cl} < \text{smooth-mix-Cl} \approx \text{smooth-all-Cl} < \text{rough-out-Cl} < \text{rough-all-Cl}$$

This trend is consistent with the structural data presented in Figure 4 which demonstrated that the solute is more strongly

TABLE 4: Values of s_{aq} for Transitions 1−4 at the Five Monolayer/Water Interfaces

monolayer	Transition 1	Transition 2	Transition 3	Transition 4
rough-all-Cl	0.90	0.90	0.83	0.91
rough-out-Cl	0.75	0.84	0.84	0.87
smooth-all-Cl	0.87	0.92	0.86	0.91
smooth-mix-Cl	0.86	0.90	0.87	0.93
rough-in-Cl	0.79	0.80	0.80	0.93
average	0.83	0.87	0.84	0.91

interacting with the rough-out-Cl and rough-all-Cl surfaces. This interaction is mainly electrostatic in nature and thus shows up in the electronic spectral shift.

(3) The differences between the spectral shifts at the different surfaces are mainly due to the different degrees of interaction between the chromophore and the organic surfaces. This is clearly shown in Table 4 where the water contribution is almost the same for all the surfaces and about 75−90% of the value in bulk water.

(4) The spectral shifts at each of the five interfaces are greater than the shifts for the same transitions in bulk water. These results indicate that these interfaces are more polar than bulk water because the contribution from the polar organic surface is greater than the 10−25% reduction in the contribution of water. These observations are in contrast to the case of water next to hydrophobic unsubstituted hydrocarbon monolayers where all the spectral shifts observed were due to the interaction with water. In that case, differences in the contribution from water between the rough and the smooth surfaces were found when the solute was covalently attached to a chain molecule making water accessibility a fundamental factor.

The finding that water next to immobile polar surfaces gives rise to an interface whose polarity is greater than that of bulk water is intriguing in light of recent experiments observing a similar effect. Zhang and Walker used second harmonic generation to probe the absorption spectrum of 4-aminobenzophenone ($\Delta\mu \approx 11.5$ D) at the interface between hydrophilic quartz and various alcohol solvents.[6] The use of various *n*-alcohol solvents results in interfaces with lower polarity relative to the bulk liquid, while the interface with a branched alcohol, 2-propanol, is more polar than the bulk liquid. Based on a surface area argument, the substrate O−H groups participate in hydrogen bonding with *n*-alcohol solvents in a 1:1 ratio, which restricts the orientation of liquid molecules relative to the bulk liquid and results in reduced dipolar solute−solvent interactions. While hydrogen bonding is not occurring in our systems, the observation of s_{aq} values less than unity is proposed to be due to the restriction of water orientation adjacent to the monolayers and this entropic effect is evident from Figure 3. In the case of 2-propanol, the surface area required to maximize hydrogen bonding is 50% greater than 1-propanol resulting in free surface O−H groups that contribute to solvation. In fact, this contribution must be greater than any reduction due to liquid ordering resulting in a more polar interface than bulk 2-propanol. This is analogous to our systems in which the contribution from the surfaces are greater than the reduction in the contribution from water relative to the bulk resulting in more polar environments than bulk water.

(5) A comparison of the different spectra for the two smooth surfaces in Figure 6 shows that a 50% reduction in the number of chlorine-terminated hydrocarbon molecules has a negligible effect on interface polarity. While the polarity of the smooth-mix-Cl surface is expected to be lower than that of the smooth-all-Cl surface, the structural considerations show the two surfaces to be very similar. By resolving the radial distribution function shown in Figure 4 for the smooth-mix-Cl surface into contributions from methyl-terminated and chlorine-terminated hydrocarbons (data not shown), it is observed that the solute is more likely to be found adjacent to chlorine-terminated hydrocarbons. The only observed decrease in the spectral shift for the smooth-mix-Cl surface relative to smooth-all-Cl occurs with Transition 3. As the solute size increases, the contribution to the solvation energy from the monolayer becomes more sensitive to reduction in the chlorine-terminated hydrocarbon density, indicating the importance of solute structural considerations at the interface. While not the focus of this paper, it is of interest to establish the relationship between the spectral shift of a solute and the surface density of chlorine-terminated hydrocarbon molecules (or hydrocarbon molecules terminated with other functional groups) by looking at a larger number of surfaces with different Cl density.

(6) A comparison of the spectral shifts of the chromophore adsorbed at the rough-out-Cl and the smooth-mix-Cl surfaces, which differ only by the length of the chlorine-terminated hydrocarbon molecules, shows that the rougher surface has a larger spectral shift. This is attributed to differing interface structures resulting in a contribution to the solvation energy from the chlorine-terminated hydrocarbon molecules 6400 cm^{-1} greater in the case of the rough-out-Cl surface for Transition 4. The explanation of this is given above in the description of the interface polarity ordering. The effect of increased polarity at rough interfaces relative to smooth interfaces has already been established at monolayer/water interfaces[8] and liquid/liquid interfaces.[42] For example, while the spectral shifts in bulk CCl_4 and nonane are the same, the greater magnitude of the spectral shift at the water/CCl_4 interface relative to the water/nonane interface is attributed to the spherical shape of CCl_4 allowing for more freedom in the orientation of interfacial molecules (and thus a rougher surface). Another example of this has been shown in the case of artificially sharp water/CCl_4 and water/1,2-dichloroethane interfaces where an external field is applied to remove surface roughness. The spectral shifts are reduced at both "sharp" interfaces relative to the normal interfaces due to a restriction in the ability of solvent molecules to approach the solute. Our current system is slightly different in that the presence of surface pockets on rough surfaces allows the solute to more closely approach the hydrocarbon terminus but the effect is similar to that previously observed.

(7) A final conclusion from Figure 6 concerns the degree to which the polar portion of the surface is interacting with the solute. The spectral shift at the rough-in-Cl surface is consistently the smallest since the solute is farthest from the dipolar portion of the monolayer. A comparison of the spectral shifts at the rough-out-Cl and the rough-in-Cl surfaces helps to elucidate the role of surface polarity: Burying the dipolar portion of the surface by almost 5 Å reduces the spectral shift anywhere from 10%−25% depending on the magnitude of the ground state dipole, with the reduction being greatest when the solute ground state dipole is the smallest. Clearly, we expect the spectral shift to further decrease when the dipolar portion of the surface is buried deeper or its magnitude reduced.

C. Continuum Electrostatic Models. It is clear from the simulation results at the chlorine-terminated self-assembled monolayers that continuum electrostatic models for the liquid/liquid interface do not apply to these systems and this is supported by experimental results at the interface between hydrophilic quartz and 2-propanol.[6] In general, the polarity experienced by a solute at a liquid/liquid interface is close to the average polarity of the bulk liquids and this is sensitive to

the solute location in the direction normal to the interface.[42] For example, at the Gibbs surface of the water/carbon tetrachloride interface, the contribution to the spectral shift from water is reduced by approximately 20% relative to bulk water (depending on the magnitude of the ground state dipole) while the contribution from carbon tetrachloride is negligible since it is nonpolar. Similarly, at the Gibbs surface of the water/1,2-dichloroethane interface, the contribution to the spectral shift from each solvent is reduced relative to the corresponding bulk liquid. The intermediate polarity observed at liquid/liquid interfaces may be attributed to thermal capillary wave fluctuations, which create a mixed solvation structure. At the water/monolayer interfaces studied here, the contribution from water is also reduced relative to the bulk due to ordering of the water near the monolayer surface. However, the contribution from the polar chlorinated monolayers is independent of the presence of water since the monolayers are solidlike and capillary fluctuations are removed. This results in a near additive effect of the two media resulting in a polarity greater than that of bulk water and shifts that are not predicted by continuum electrostatic theory for the liquid/liquid interface. In general, the polarity at water/monolayer interfaces is predicted to exhibit an intrinsic contribution from the monolayer, depending on its polarity, plus a contribution from the adjacent liquid, which is reduced relative to the bulk liquid due to intermolecular interactions with the monolayer surface.

Since the contribution to the spectral shift from water in these systems is only reduced by 10−25% relative to bulk water, better agreement is expected with continuum electrostatic models for bulk liquids and reasonable agreement has been shown with methyl-terminated monolayer/water interfaces.[8] Continuum electrostatic models for the bulk predict the shift in the spectrum based on the dielectric constant of the liquid and the ground- and excited-state dipoles of the solute. For a parallel transition in a polar nonpolarizable liquid, the spectral shift relative to the gas phase is given by[50,51]

$$\Delta\omega = \frac{4\mu_g(\mu_g - \mu_e)}{a_o^3}\frac{\epsilon - 1}{\epsilon + 2} \qquad (12)$$

where ϵ is the static dielectric constant of the liquid, a_o is the radius of the solute cavity and μ_g and μ_e are the magnitudes of the dipole in the ground and excited states, respectively. The effect of a 33% increase in the overall change in dipole due to ground-state charge magnitude is determined by comparing Transition 2 to Transition 1. Equation 12 predicts an increase by a factor of $0.667/0.5 \times (0.667-0.0)/(0.5-0.0) = 1.8$ (charge magnitude factor) which is in excellent agreement with the range of 1.7−1.9 observed from the simulations. Comparing Transition 3 to Transition 1 tests the effect of a 33% increase in the overall change in dipole due to the increase in the ground-state bond length. The simulation results show a much smaller increase in the spectral shift than the case where the 33% increase was due to the increase in the charge magnitude. In fact, the increase observed from the simulations for Transition 3 relative to Transition 1 is in the range of 1.0−1.2 while eq 12 actually predicts a decrease by a factor of the charge magnitude factor, 1.8, multiplied by $(6/8)^3$, which yields 0.8. The discrepancy between eq 12 and the simulation results is resolved by making a final comparison between Transition 2 and 3, which tests the effect of changing only cavity size. Equation 12 predicts a decrease by a factor of $(6/8)^3 = 0.4$ while the simulation results are in the range of 0.6−0.8. These results indicate that while an increase in the spectral shift due to increasing ground-state charge magnitude is well described at the monolayer/water interface by continuum electrostatic theory for bulk liquids, an increase in the ground-state size is not predicted as well. This is due to an overestimation of the decrease in polarity experienced by a solute with a larger cavity size, which is reasonable since the spectral shifts indicate these interfaces are more polar than bulk water. The theory does not account for contribution from an adjacent polar media or ordering of water near the interface. Given that eq 12 is intended for application to bulk liquids, the systems studied are described with reasonable agreement.

V. Conclusions

The interface between water and self-assembled hydrocarbon monolayers whose terminal methyl groups have been partially or completely substituted by chlorine atoms represents an interesting system that is at the border between a liquid/liquid and a liquid/solid interface. As in the case of a liquid/liquid interface, surface roughness plays an important role in determining interface polarity and, like some liquid/solid interfaces, the effective polarity of the interface is greater than that of the bulk liquid. The study of these surfaces has the advantage of greater control over the detailed structure than at the liquid/liquid interface and provides unique insight into the nature of intermolecular interactions at liquid/liquid and liquid/solid interfaces.

Acknowledgment. This work has been supported by a grant from the National Science Foundation (CHE-9981847).

References and Notes

(1) Benjamin, I. *Annu. Rev. Phys. Chem.* **1997**, *48*, 401.
(2) Benjamin, I. *Chem. Rev.* **1996**, *96*, 1449.
(3) Eisenthal, K. B. *Chem. Rev.* **1996**, *96*, 1343.
(4) Richmond, G. L. *Annu. Rev. Phys. Chem.* **2001**, *52*, 357.
(5) Wang, H.; Borguet, E.; Eisenthal, K. B. *J. Phys. Chem.* **1997**, *101*, 713.
(6) Zhang, X.; Walker, R. A. *Langmuir* **2001**, *17*, 4486.
(7) Rudich, Y.; Benjamin, I.; Naaman, R.; Thomas, E.; Trakhtenberg, S.; Ussyshkin, R. *J. Phys. Chem. A* **2000**, *104*, 5238.
(8) Squitieri, E.; Benjamin, I. *J. Phys. Chem. B* **2001**, *105*, 6412.
(9) Whitesides, G. M.; Laibinis, P. E. *Langmuir* **1991**, *6*, 87.
(10) Giancarlo, L. C.; Flynn, G. W. *Annu. Rev. Phys. Chem.* **1998**, *49*, 297.
(11) Brunner, H.; Vallant, T.; Mayer, U.; Hoffmann, H. *Surf. Sci.* **1996**, *368*, 279.
(12) Lu, J. R.; Thomas, R. K. *J. Chem. Soc., Faraday Trans.* **1998**, *94*, 995.
(13) Olbris, D. J.; Ulman, A.; Shnidman, Y. *J. Chem. Phys.* **1995**, *102*, 6865.
(14) Eisert, F.; Dannenberger, O.; Buck, M. *Phys. Rev. B* **1998**, *58*, 10860.
(15) Evans, D.; Wampler, R. *J. Phys. Chem. B* **1999**, *103*, 4666.
(16) Kaschak, D. M.; Mallouk, T. E. *J. Am. Chem. Soc.* **1996**, *118*, 4222.
(17) Hautman, J.; Bareman, J. P.; Mar, W.; Klein, M. L. *J. Chem. Soc., Faraday Trans.* **1991**, *87*, 2031.
(18) Stouch, T. R. *Mol. Simul.* **1993**, *10*, 335.
(19) Venable, R. M.; Zhang, Y. H.; Hardy, B. J.; Pastor, R. W. *Science* **1993**, *262*, 223.
(20) Marrink, S. J.; Berkowitz, M.; Berendsen, H. J. C. *Langmuir* **1993**, *9*, 3122.
(21) Mar, W.; Klein, M. L. *Langmuir* **1994**, *10*, 188.
(22) Pohorille, A.; Wilson, M. A. *Origins of Life and Evolution of the Biosphere* **1994**, *25*, 21.
(23) Schulten, K.; Zhou, F. *J. Phys. Chem.* **1995**, *99*, 2194.
(24) Tobias, D. J.; Tu, K. C.; Klein, M. L. *Curr. Opin. Colloid Interface Sci.* **1997**, *2*, 15.
(25) Hansen, J.-P.; McDonald, I. R. *Theory of Simple Liquids*, 2nd ed.; Academic: London, 1986.
(26) Dang, L. X.; Rice, J. E.; Caldwell, J.; Kollman, P. A. *J. Am. Chem. Soc.* **1991**, *113*, 2481.
(27) Tsun-Mei, C.; Dang, L. X.; Peterson, K. A. *J. Phys. Chem. B* **1997**, *101*, 3413−3419.

(28) Dang, L. X.; Chang, T. *J. Phys. Chem. B* **2002**, *106*, 235.
(29) Jungwirth, P.; Tobias, D. J. *J. Phys. Chem. A* **2002**, *106*, 379.
(30) Benjamin, I. *Chem. Phys. Lett.* **1998**, *287*, 480.
(31) Lagutchev, A. S.; Song, K. J.; Huang, J. Y.; Yang, P. K.; Chuang, T. J. *Surf. Coat. Technol.* **1997**, *94*−*95*, 383.
(32) Weiner, S. J.; Kollman, P. A.; Nguyen, D. T.; Case, D. A. *J. Comput. Chem.* **1986**, *7*, 230.
(33) Jorgensen, W. L. *J. Am. Chem. Soc.* **1981**, *103*, 335.
(34) Burkert, U.; Allinger, N. L. *Molecular Mechanics*; American Chemical Society: Washington, DC, 1982.
(35) Benjamin, I. *J. Chem. Phys.* **1992**, *97*, 1432.
(36) Berendsen, H. J. C.; Postma, J. P. M.; Gunsteren, W. F. V.; Hermans, J. In *Intermolecular Forces*; Pullman, B., Ed.; D. Reidel: Dordrecht, 1981; p 331.
(37) Kuchitsu, K.; Morino, Y. *Bull. Chem. Soc. Jpn.* **1965**, *38*, 814.
(38) Ciccotti, G.; Ferrario, M.; Hynes, J. T.; Kapral, R. *Chem. Phys.* **1989**, *129*, 241.
(39) Reichardt, C. *Chem. Rev.* **1994**, *94*, 2319.
(40) Allen, M. P.; Tildesley, D. J. *Computer Simulation of Liquids*; Clarendon: Oxford, 1987.
(41) Hautman, J.; Klein, M. L. *Mol. Phys.* **1992**, *75*, 379.
(42) Michael, D.; Benjamin, I. *J. Chem. Phys.* **1997**, *107*, 5684.
(43) Linse, P. *J. Chem. Phys.* **1987**, *86*, 4177.
(44) Meyer, M.; Mareschal, M.; Hayoun, M. *J. Chem. Phys.* **1988**, *89*, 1067.
(45) Benjamin, I. Molecular dynamics simulations in interfacial electrochemistry. In *Modern Aspects of Electrochemistry*; Bockris, J. O. M., Conway, B. E., White, R. E., Eds.; Plenum Press: New York, 1997; Vol. 31, p 115.
(46) Chang, T. M.; Dang, L. X. *J. Chem. Phys.* **1996**, *104*, 6772.
(47) Pohorille, A.; Wilson, M. A. *J. Mol. Struct. (THEOCHEM)* **1993**, *103*, 271.
(48) Wang, H.; Eisenthal, K. B. *Abstract, Fall ACS National Meeting*, 1997.
(49) Wang, H. F.; Borguet, E.; Eisenthal, K. B. *J. Phys. Chem. B* **1998**, *102*, 4927.
(50) McRae, E. G. *J. Phys. Chem.* **1957**, *61*, 562.
(51) Bakhshiev, N. G. *Opt. Spektrosk.* **1964**, *16*, 821.